



Published in final edited form as:

Sci Signal. ; 12(590): . doi:10.1126/scisignal.aaw7095.

Galectin-3 initiates epithelial-stromal paracrine signaling to shape the proteolytic microenvironment in corneal repair

Dina B. AbuSamra, Jérôme Mauris, Pablo Argüeso*

Schepens Eye Research Institute of Massachusetts Eye and Ear, Department of Ophthalmology, Harvard Medical School, Boston, MA 02114, USA.

Abstract

Paracrine interactions between epithelial cells and stromal fibroblasts occur during tissue repair, development, and cancer. Crucial to these processes is the production of matrix metalloproteinases (MMPs) that modify the microenvironment. Here, we demonstrated that the carbohydrate-binding protein galectin-3 stimulates microenvironment remodeling in the cornea by promoting the paracrine action of secreted interleukin-1 β (IL-1 β). By using in vitro live cell imaging, we observed rapid activation of the *MMP9* promoter in clusters of cultured human epithelial cells after direct heterotypic contact with single primary human fibroblasts. Soluble recombinant galectin-3 and endogenous galectin-3 of epithelial origin were both fully capable of inducing MMP9 activity through the induction of IL-1 β secretion by fibroblasts. In vivo, mechanical disruption of the basement membrane in wounded corneas prompted an increase in the abundance of IL-1 β in the stroma and increased the amount of gelatinase activity in the epithelium. Moreover, corneas of galectin-3-deficient mice failed to stimulate IL-1 β following wounding. This mechanism of paracrine control has broad importance for our understanding of how the proteolytic microenvironment is modified in epithelial-stromal interactions.

Abstract

One-Sentence Summary: Epithelia-fibroblast contact promotes paracrine signaling that stimulates matrix remodeling during corneal repair.

Editor's Summary: Epithelial-stromal paracrine signaling for cornea repair

Injuries to epithelia that breach the basement membrane allow epithelial cells to come into contact with the underlying stroma. Epithelial-stromal interactions are critical for matrix remodeling and repair of the damaged tissue. AbuSamra *et al.* found that contact with corneal fibroblasts stimulated corneal epithelial cells to produce the matrix metalloprotease MMP9. The

*Corresponding author. pablo_argueso@meei.harvard.edu.

Author contributions:

D.B.A. contributed to study design, collected and analyzed data, and wrote the manuscript. J.M. contributed to study design, collected and analyzed data, and revised the manuscript. P.A. supervised the study, contributed to study design and data analysis, and finalized the manuscript.

Competing interests: The authors declare that they have no competing interests.

Data and materials availability: Plasmids and the newly created epithelial MMP9 promoter reporter cell line described herein are available from Schepens Eye Research Institute with a materials transfer agreement. The PCR array data have been deposited into the Harvard Dataverse (<https://doi.org/10.7910/DVN/UQRQ30>) with accession number UQRQ30. All other data needed to evaluate the conclusions in the paper are present in the paper or in the Supplementary Materials.

carbohydrate-binding protein galectin-3 from epithelial cells stimulated fibroblasts to produce the pro-inflammatory cytokine IL-1 β , which in turn stimulated *MMP9* expression in the epithelial cells. This paracrine signaling network was required for the healing of corneal wounds in vivo only if the wounds breached the basement membrane. Because galectin-3 is associated with various tissue remodeling events, this galectin-3–induced epithelial-stromal paracrine network may also be relevant in other pathophysiological contexts in which microenvironment remodeling plays a critical role, such as cancer cell invasion and metastasis.

INTRODUCTION

Reciprocal interactions between epithelial cells and neighboring stromal fibroblasts are centerpieces of tissue repair, embryonic development, tumor growth, and metastasis (1, 2). A common form of communication between these cells involves the production and secretion of paracrine signals, such as growth factors and cytokines, that initiate changes in cellular behavior and transform the local microenvironment. Of importance during this process are extracellular proteases that remodel cell surfaces and the extracellular matrix, thereby influencing the proliferation, motility, recruitment, and differentiation of cells (3). Both epithelial cells and fibroblasts produce large amounts of matrix-degrading enzymes following the establishment of heterotypic cellular interactions, but the precise paracrine mechanisms responsible for the stimulation of these proteases remain mostly uncharacterized.

Matrix metalloproteinases (MMPs) are zinc-dependent endopeptidases responsible for tissue remodeling in both physiological and pathological conditions. Two members of this family, the gelatinases MMP2 and MMP9, contain a fibronectin-like domain within the catalytic domain that allows binding to and degradation of denatured collagens, in particular basement membrane type IV and anchoring fibril type VII collagens (4). These functionally related proteases are synthesized and secreted by various cell types including fibroblasts and endothelial, inflammatory, and epithelial cells. The expression of the genes encoding these proteases appears to be differentially regulated based on the presence of distinct promoter regions within each gene (5). This is illustrated by the action of growth factors and proinflammatory cytokines, such as epidermal growth factor (EGF), interleukin-1 β (IL-1 β), and tumor necrosis factor α (TNF α), which more efficiently stimulate *MMP9* compared to *MMP2* (6). Experiments in several animal model systems have demonstrated that MMP9 is crucial for the organization of the collagen matrix in the context of acute and chronic tissue damage (7, 8). In cornea, MMP9 of epithelial origin coordinates the removal of the fibrinogen provisional matrix and participates in the assembly of new basement membrane following injury (9, 10).

Galectin-3 is a β -galactoside-binding protein composed of an evolutionarily conserved carbohydrate recognition domain and a large amino-terminal region. The ability of the latter to promote self-aggregation is critical for the biological function of galectin-3. By controlling the clustering and endocytosis of cell surface receptors, galectin-3 exerts important regulatory actions in many signaling pathways (11). One important characteristic of this lectin is that it is associated with various conditions that require microenvironmental control. It is abundantly synthesized by the migrating epithelium during wound repair, and

its stimulation in tumor cells has been linked to the invasion-metastasis cascade (12, 13). Here, we describe a previously unknown function of galectin-3 in sustaining a proteolytic microenvironment when epithelial-stromal interactions are initiated. We show that single fibroblasts activated the *MMP9* promoter in clustered epithelial cells following the induction of direct heterotypic cell-cell contacts. We further demonstrated that this effect was mediated by galectin-3 of epithelial origin and involved the activation of a fibroblast-dependent paracrine mechanism of IL-1 β secretion. These results highlight the importance of carbohydrate-binding proteins in modulating paracrine signaling in pathophysiological settings.

RESULTS

Contact with single fibroblasts activates the *MMP9* promoter locally in epithelia

Molecular crosstalk between epithelial cells and fibroblasts in adjacent stromal compartments is known to provide signals essential to the production of proteolytic enzymes and the modification of the local microenvironment (14, 15). To better understand the signaling pathways responsible for the production of matrix-degrading enzymes following heterotypic cell-cell contacts, we constructed an enhanced green fluorescent protein (eGFP) reporter system to monitor the activation of the *MMP9* promoter in a telomerase-immortalized human corneal epithelial cell line (fig. S1, A and B). Confluent cultures of the promoter reporter cell line were separated from primary cultures of primary human corneal stromal fibroblasts using a permeable agarose divider and subjected to time-lapse video microscopy. Removal of the divider allowed visualization of migrating fibroblasts with extending lamellipodia at the leading edge of the cells (Fig. 1A). Strikingly, direct contact of single fibroblasts with the epithelial sheet promoted the rapid and simultaneous activation of the *MMP9* promoter reporter in immediately adjacent clusters of epithelial cells (Fig. 1A and Movie S1).

Next, we assessed the ability of the cultures to secrete MMP9 in a mixed coculture system. We found that prompting direct heterotypic cell-cell contacts increased the abundance of MMP9 in the conditioned media as judged by gelatin zymography (Fig. 1B). The accumulation of MMP9 was time-dependent and was maximal at 48 h. The abundance of *MMP9* mRNA was also significantly higher following the establishment of direct heterotypic contact compared to homotypic conditions (Fig. 1C). Consistent with our in vitro live-cell imaging data, we found that the relative number of fibroblasts in the coculture system had a profound effect on MMP9 production. Increasing the ratio of fibroblasts to epithelial cells from 1:100 to 1:1 resulted in a striking increase in the secretion of MMP9 into the media (Fig. 1D). We confirmed that the abundance of secreted MMP9 in coculture experiments was directly proportional to the number of fibroblasts in coculture experiments using a telomerase-immortalized human corneal fibroblast cell line (Fig. 1E).

Galectin-3 prompts reciprocal signaling and influences epithelial MMP9 secretion

To determine whether the induction of MMP9 activity in epithelial cells was dependent on the juxtacrine interaction with adjacent fibroblasts, we treated epithelial cells with plasma membrane fractions isolated from primary fibroblasts. In these experiments, we also

included the corresponding cytosolic fractions. Analysis of the results indicated that the amount of MMP9 produced under these conditions was marginal compared to that observed in the mixed coculture system (fig. S2, A and B). We also found that inhibition of N-glycosylation in corneal fibroblasts by deoxymannojirimycin did not significantly alter the levels of MMP9 in coculture conditions (fig. S3). We next examined whether factors in the conditioned media of fibroblasts were responsible for the induction of MMP9 activity in epithelial cells. Using the epithelial *MMP* promoter reporter cell line, we found that conditioned media obtained from quiescent fibroblasts grown alone failed to induce *MMP9* promoter activity (Fig. 2A). On the other hand, conditioned media obtained from heterotypic cultures successfully stimulated the *MMP9* promoter in parallel homotypic cultures of epithelial cells, indicating that critical paracrine factors were being secreted after the establishment of direct heterotypic cell-cell contacts.

Because galectin-3 is a protein that increases in abundance across a range of environmental conditions associated with the remodeling of the extracellular matrix, we sought to determine whether galectin-3 was involved in the activation of fibroblasts in our experiments. To this purpose, we incubated primary cultures of human corneal fibroblasts with 100 µg/ml full-length recombinant human galectin-3. The conditioned media was then depleted of galectin-3 by lactose-affinity chromatography and applied to epithelial cells. As shown by gelatin zymography, exogenous galectin-3, but not a bovine serum albumin control, prompted fibroblasts to produce secreted factors that triggered epithelial MMP9 secretion (Fig. 2B). Further examination of the function of endogenous proteins in promoting MMP9 activity pointed to galectin-3 of epithelial origin as a major player. In these experiments, coculture of fibroblasts with epithelial cells treated with a small interfering RNA (siRNA) targeting galectin-3 resulted in a significant decrease in MMP9 secretion compared to epithelial cells treated with a scrambled control siRNA (Fig. 2C). This impairment in MMP9 secretion was, on the other hand, not observed when galectin-3–depleted fibroblasts were used in the coculture system (Fig. 2D). Overall, these data support a prominent role for epithelial galectin-3 in promoting paracrine signaling between epithelial cells and stromal fibroblasts that results in the expression of *MMP9* in epithelial cells.

IL-1 β acts as a galectin-3–induced paracrine signal in fibroblasts

To identify potential paracrine signals that fibroblasts produce in response to galectin-3, we employed a real-time PCR array with primers for 84 genes involved in the inflammatory response (Fig. 3A and Table S1). We compared the expression profiles of these genes in unstimulated fibroblast monocultures to two different conditions that result in MMP9 secretion: direct heterotypic cell-cell contacts between epithelia and fibroblasts and the addition of 100 µg/ml soluble exogenous galectin-3 to fibroblast monocultures. Direct cell-cell contact evoked an increase in *IL1a*, *IL1b*, *IL6*, *IL18*, and *CXCL10* expression and a decrease in *CCL7*, *LY96* and *KNG1* expression. Stimulation of fibroblasts with soluble galectin-3 increased the expression of *IL1b*, *CCL5*, *CXCL3*, and *CXCL10*. Comparison of the two sets of data revealed that *IL1b* and *CXCL10*, both of which encode pro-inflammatory cytokines, were the only two genes induced by both methods of fibroblast stimulation (Fig. 3B). In addition to the increase in *IL1 β* and *CXCL10* transcripts, the total amount of IL-1 β and CXCL10 proteins also increased in the conditioned media of

fibroblasts stimulated with epithelial cells or soluble galectin-3 as measured by ELISA (Fig. 3C).

We next determined whether galectin-3 of epithelial origin was capable of triggering IL-1 β and CXCL10 responses after the establishment of direct heterotypic cell-cell contacts. Here, siRNA-mediated depletion of endogenous galectin-3 in epithelial cells reduced the abundance of IL-1 β in the cell culture media (Fig. 3D), supporting a role for epithelial galectin-3 in inducing the production and secretion of IL-1 β by fibroblasts, presumably by binding to fibroblast receptors that stimulate signaling leading to *IL1b* expression. Conversely, unlike soluble galectin-3, galectin-3 of epithelial origin did not influence the abundance of CXCL10 (Fig. 3D), perhaps as a result of differential presentation or the relative concentration of galectin-3 in the plasma membrane of epithelial cells, which might not be sufficient to activate the CXCL10 pathway in fibroblasts.

It is well established that, in the presence of carbohydrate ligands, galectin-3 polymerizes through its N-terminal domain, resulting in the formation of lattice-like structures on plasma membranes that are essential for the biological activity of the cell (16). Use of a mutant lacking the N-terminal polymerization domain further supported that galectin-3 binding and multimerization was necessary to induce IL-1 β secretion by corneal fibroblasts (fig. S3). Disrupting the processing of highly N-glycosylated receptors did not significantly alter the abundance of MMP9 in cocultures (fig. S4), indicating that galectin-3 in cornea induces paracrine signaling and alters the proteolytic microenvironment through a mechanism independent of ligands processed through the N-glycan branching pathway.

Multiple cytokines, including IL-1 β , can activate the *MMP9* promoter (17). To determine whether fibroblast-produced IL-1 β was involved in stimulating MMP9 secretion in a manner that depended on galectin-3, we depleted IL-1 β in fibroblasts and asked whether that impaired MMP9 secretion in epithelial cells. By ELISA, we found negligible amounts of IL-1 β in the cell culture media of quiescent fibroblasts. For that reason, we treated the fibroblasts with soluble galectin-3 in control experiments to demonstrate that delivery of an siRNA targeting IL-1 β efficiently reduced the secretion of the cytokine (Fig. 3E). We then confirmed that conditioned media from fibroblasts treated with a scrambled control siRNA then stimulated with soluble galectin-3 was sufficient to induce MMP9 secretion in epithelial cells (Fig. 3F). Most importantly, we found that conditioned media of IL-1 β -depleted fibroblasts treated with soluble galectin-3 did not support the induction of MMP9 in epithelial cells. Overall, these in vitro data indicate that epithelial galectin-3 modifies the proteolytic microenvironment by promoting IL-1 β secretion in fibroblasts.

The basement membrane protects against galectin-3–induced IL-1 β signaling

Basement membranes are thin extracellular matrices that separate tissue compartments and, because of their high content of type IV collagen, protect them from mechanical strain (18). Alteration of basement membranes due to trauma or tissue remodeling events results in the establishment of direct heterotypic cell-cell contacts. To determine whether the basement membrane plays a role in regulating galectin-3–induced IL-1 β signaling, we used two animal models of mechanical cornea injury that differentially affect the integrity of the basement membrane (19). Debridement wounding with a dulled blade results in the removal

of the epithelium while preserving the basement membrane, whereas wounding performed with a rotating burr removes the basement membrane and reaches deeper areas of the anterior stroma (Fig. 4A). In our experiments, we used anterior segment optical coherence tomography at the time of injury to confirm that the corneal thickness decreased following epithelial debridement and that the wound was deeper when using a rotating burr compared to debridement (Fig. 4B). By 14–16 h after injury, the debridement wounds made with a dulled blade were closed, as shown by topical instillation of fluorescein stain, but those performed with the rotating burr were not (Fig. 4C).

Immunolocalization of laminin α -1 confirmed that the basement membrane was mostly absent in the central cornea 14–16 h after injury with a rotating burr, with some discrete staining in the periphery (Fig. 4D). Of note, there were few stromal cells in the central cornea, likely as a consequence of early apoptotic events known to occur after extensive corneal injury (20). The evaluation of consecutive tissue sections revealed the presence of vimentin-positive cells in the peripheral stroma in close proximity to the basal cell layer of the epithelium in rotating burr wounds (Fig. 4D), suggesting the existence of epithelial-mesenchymal cell interactions. Consistent with our *in vitro* data indicating that direct heterotypic cell-cell contacts promoted MMP9 activity, we found increased gelatinolytic activity in epithelial cells located at the peripheral region of the rotating burr wounds, as shown by *in situ* gelatin zymography (Fig. 4D). Wounds in the debridement injury model, on the contrary, were characterized by the presence of a continuous basement membrane, the absence of stromal cells in close proximity to the epithelial cells, and a more rapid restoration of the epithelial layer with negligible gelatinolytic activity at the time of closure (Fig. 4D).

Overall, the two models of corneal injury induced quite different responses 14–16 h after wounding. We took advantage of these results to determine the role of the basement membrane in protecting against galectin-3–induced IL-1 β signaling. The abundance of IL-1 β in the stromal compartment of corneas from wild-type mice significantly increased after application of a rotating burr compared to unwounded tissue or corneas that underwent a dulled blade injury (Fig. 4, E–F). Strikingly, this gain in IL-1 β content was completely absent in the corneal stroma of galectin-3–deficient mice after wounding (Fig. 4, E–F). Concomitantly, we observed minimal gelatinolytic activity in epithelial cells located at the peripheral region of rotating burr wounds in galectin-3–deficient mice (Fig. 4G). In summary, these *in vivo* results illustrate the importance of galectin-3 in modulating the IL-1 β signaling responses that follow the disruption of the basement membrane.

DISCUSSION

Over five decades ago, Grillo and Gross proposed that interaction between epithelial cells and neighboring fibroblasts during mammalian wound repair could account for the synthesis of proteases responsible for the breakdown of the extracellular matrix (21). Since then, additional work, particularly in the context of tumor progression, has identified a prominent role for secreted cytokines and growth factors in the regulation of protease activity through complex autocrine and paracrine mechanisms (15, 22). Surprisingly, relatively little attention has been devoted to the molecules that initiate such signaling modalities following direct

heterotypic cell-cell contact. Here, we reveal a direct role for galectin-3 in regulating the proteolytic microenvironment in epithelial-stromal interactions by promoting the paracrine action of secreted IL-1 β (Fig. 5).

The main function of matrix-degrading enzymes in epithelial and stromal compartments is to maintain physiological turnover. Thus, they are commonly present in the latent form and in low amounts in healthy tissues (23). Their abundance greatly increases under conditions that require tissue remodeling, such as trauma, tissue morphogenesis, or oncogenic transformation. Many of the proteases produced in the stromal compartment originate from fibroblasts, inflammatory cells, and endothelial cells, which respond to juxtacrine and paracrine signals produced by the epithelial cells (24). Conversely, epithelial cells can also function as the source of matrix-degrading enzymes when present in close proximity to fibroblasts. In this context, they contribute to alter the local microenvironment, particularly through modification of the basement membrane (9, 10, 23).

The contribution of carbohydrate-binding proteins to the epithelial-stromal interaction has not been fully explored. It has been shown that galectin-3 from pancreatic ductal adenocarcinoma promotes the production of IL-8, CXCL1, and CCL2 in pancreatic stellate cells by integrin signaling, resulting in an aggressive malignant phenotype (25). In our study, we observed that galectin-3 of epithelial origin stimulated IL-1 β in corneal fibroblasts, resulting in the modification of the proteolytic microenvironment. The causes for the distinctive paracrine response to galectin-3 stimulation in terms of cytokine and chemokine expression likely depend on the target tissue and its pathological state. IL-1 β is an important mediator of inflammation and tissue damage in cornea. Under homeostatic conditions, IL-1 β is primarily present in the corneal epithelial compartment in equilibrium with the IL-1 receptor antagonist, which favors a protective environment (26, 27). Moreover, galectin-3 does not promote IL-1 β production in these quiescent corneal epithelial cells (28). Injury to the epithelium and rupture of the basement membrane, on the other hand, prompts a rapid accumulation of IL-1 β in the corneal stroma and, consequently, the initiation of responses crucial to the degradation and remodeling of the collagenous extracellular matrix (26, 29, 30). Despite advances in understanding the response of epithelial surfaces to IL-1 β stimulation, much remains to be discovered with regard to the mechanisms that regulate its production. Previous research has indicated a critical function for galectin-3 in selectively promoting cytokine production in fibroblasts (31). However, these contributions have rarely been examined in the context of direct heterotypic cell-cell contacts. Given that galectin-3 is significantly increased in areas of extensive remodeling in both ocular and non-ocular tissues, it is plausible to envision a critical regulatory function for this lectin in promoting paracrine signaling during these processes in various tissues.

An outstanding question remains over the identity of the surface receptors on fibroblasts that respond to galectin-3 following the establishment of direct heterotypic contact. Galectin-3 has been implicated in promoting cytokine secretion in tissue fibroblasts by activation of numerous pathways such as the Toll-like receptor, nuclear factor κ B (NF- κ B), and mitogen-activated protein (MAP) kinase (31–33). In lung fibroblasts, the stimulating effect of galectin-3 appears to derive from its ability to interact with cell surface glycoconjugates (34). We initially speculated that highly N-glycosylated receptors could act as potential

targets in corneal fibroblasts. Their modification by N-acetylglucosaminyltransferase V, a Golgi enzyme responsible for the biosynthesis of poly-N-acetyllactosamine sequences recognized by galectin-3, has been shown to regulate cytokine signaling (35). However, in our hands, disruption of complex N-glycan processing in corneal fibroblasts by the mannosidase inhibitor deoxymannojirimycin did not significantly alter the levels of MMP9 in coculture conditions. These results were not completely unexpected because previous studies in other cell types, such as diffuse large B-cell lymphoma cells (36) and CD8⁺ T cells (37), have shown that complex N-glycans are not always essential for galectin binding to their ligands. Thus, it is feasible that galectin-3 in cornea induces paracrine signaling and alters the proteolytic microenvironment through a mechanism that is independent of the N-glycan branching pathway. Several alternative modalities of galectin-3 interaction with surface receptors have been established, including recognition of O-glycans and gangliosides (38–40). Defining the specific receptors responsible for the activation of corneal fibroblasts by galectin-3 merits further investigation.

In conclusion, the studies described herein provide evidence for the concept that galectin-3–induced paracrine signaling is a key regulator of the proteolytic microenvironment in epithelial-stromal interactions. The findings highlight the importance of increased galectin-3 abundance in biological systems undergoing tissue remodeling and provide great potential for manipulating signaling events that enable the degradation of extracellular matrices.

MATERIALS AND METHODS

Cell Culture

Human fibroblasts were derived from eye bank donor corneas with the approval of the Institutional Review Board of the Massachusetts Eye and Ear Human Studies Committee. Primary cultures were prepared as previously described by allowing the cells to adhere to the bottom of tissue culture plates in the presence of Dulbecco's Modified Eagle Medium / Nutrient Mixture F12 (DMEM/F12; GE Healthcare) supplemented with 10% newborn calf serum (41). Telomerase-immortalized human corneal epithelial cells (42) and telomerase-immortalized human corneal fibroblasts (43) were grown in keratinocyte serum-free medium (Thermo Fischer Scientific) or DMEM/F12 supplemented with 10% newborn calf serum, respectively. Cells in the mixed coculture system were incubated at 1:1 ratio, unless otherwise specified, in DMEM/F12 supplemented with 10% newborn calf serum prior to experimental assays.

For inhibition of N-glycosylation, primary human corneal fibroblasts (2.5×10^3 cells/cm²) were treated with or without 5 mM deoxymannojirimycin for 48 h. After washing with sterile PBS, epithelial cells (10^5) were added to the cell culture in serum-free conditions.

Animal Experiments

All animal-based procedures conformed to the Association for Research in Vision and Ophthalmology statement for the Use of Animals in Ophthalmic and Vision Research. The experimental protocols were approved by the Animal Care Committee of the Massachusetts Eye and Ear Infirmary. C57BL/6J and galectin-3-deficient mice (strain B6.Cg-

Lgals3^{tm1Poi/J}) were obtained from The Jackson Laboratory. To produce corneal wounds, 8 to 12-week-old mice were anesthetized intraperitoneally with a 1:1 mixture of ketamine (120 mg/kg) and xylazine (20 mg/kg). Proparacaine hydrochloride ophthalmic solution was applied to the cornea as a topical anesthetic. A 2-millimeter area was demarcated in the central cornea with a trephine before the wounding. A dulled blade held by a blade breaker was gently used to remove the epithelium and preserve the basement membrane from within the marked area on the right eye of each mouse as described (19). A rotating burr (Algerbrush II, The Alger Companies) was used to remove the basement membrane and reach the anterior corneal stroma (44). After wounding, eyes were treated with vetropolycin ophthalmic ointment (Dechra) to minimize superficial infections of the ocular surface. Images of the anterior segment were taken following injury by anterior segment optical coherence tomography (Envisu R2210, Bioptigen) to determine corneal thickness. Corneas were allowed to heal in vivo for 14–16 h.

MMP9 Reporter Construct

A cell line was generated by transfection of telomerase-immortalized human corneal epithelial cells with a human *MMP9* promoter reporter construct. The *MMP9* promoter sequence (–1317 to +21 region relative to the transcription start site) cloned into the lentiviral vector pEZX-LvPF02 directly upstream of an eGFP coding sequence was purchased from Genecopoeia (product ID: HPRM45843). The vector was cotransfected into 293T cells with the psPAX2 and the pCMV-VSV-G packaging system (10:10:1 ratio) using Lipofectamine 2000 (Invitrogen) according to the manufacturer's instructions. After 24 h, the DNA-Lipofectamine mixture was removed and the media replaced with DMEM/F12 supplemented with 30% fetal bovine serum and 15 mM HEPES. The lentiviral particles were harvested at 48 and 72 h post transfection and pooled. The titer was determined by transducing corneal epithelial cells with serial dilutions of the viral supernatant in 10 µg/mL of polybrene. The number of cells expressing eGFP was determined using fluorescence-activated cell sorting. The viral titer, calculated as transduction units per ml (number of cells × percent of fluorescent cells × dilution factor / transduction volume in ml), was 5.5×10^6 . Corneal epithelial cells were transduced at a multiplicity of infection of 11. Fluorescence was read at an excitation wavelength of 485 nm and an emission wavelength of 530 nm using a Synergy 2 Multi-Detection Microplate Reader (BioTek).

Time-lapse Video Microscopy

Cocultures of fibroblasts and epithelial cells were imaged live using a Leica DMI6000 B inverted microscope (Leica Microsystems). The cell types were grown separately in the presence of a permeable agarose divider as previously described (45). The divider was removed upon confluence in both compartments and the cells were allowed to interact in DMEM-F12 media supplemented with 10% newborn calf serum. An environment of 5% CO₂ and 37°C was maintained in an enclosed chamber during the recording. Time-lapse phase-contrast and fluorescence images were captured simultaneously with a 10x objective lens at 20-min intervals over a period of 48 h. The collected images were converted to .avi files using ImageJ software (National Institutes of Health).

Immunofluorescence Microscopy

Mouse eyes were frozen in optimal cutting temperature compound for sectioning using a cryostat. Tissue sections (10 μm) on glass slides were fixed in paraformaldehyde (IC fixation buffer, Thermo Fischer Scientific) for 20 min at room temperature. After washing with phosphate-buffered saline (PBS), nonspecific binding was blocked by incubation with 3% bovine serum albumin (BSA) and 5% goat serum in PBS for 1 h. Slides were then incubated with primary antibodies against laminin- α 1 (10 $\mu\text{g/ml}$; AL-4, R&D Systems) or vimentin (10 $\mu\text{g/ml}$; D21H3, Cell Signaling Technology) in blocking buffer for 2 h. Samples were washed and treated with the appropriate Alexa Fluor 568-conjugated secondary antibodies at 10 $\mu\text{g/ml}$ for 1 h. Slides were finally mounted in VectaShield mounting medium containing DAPI (Vector Laboratories) and photographed on a Zeiss Axio Observer Z1 inverted fluorescent microscope (Carl Zeiss Microimaging). Incubation with primary antibodies was routinely omitted in control experiments.

Gelatin and In Situ Zymography

Serum-free conditioned media were collected and centrifuged at 13,000 g for 30 min to remove cells and cellular debris. The supernatant (2–10 μl) was mixed with non-reducing loading buffer (50 mM Tris-HCl, pH 6.8, 4% glycerol, 0.8% SDS, and 0.1% bromophenol blue) and electrophoresed on 7.5% SDS-PAGE gels containing 1 mg/ml gelatin (bovine skin type B). Gels were maintained overnight in 50 mM Tris-HCl, pH 7.5 containing 5 mM CaCl_2 and 2.5% Triton X-100. After washing with distilled water, gels were incubated for 24 h at 37°C in the above buffer without Triton X-100 so that reactivation of the enzyme would occur. Gels were stained in Coomassie brilliant blue solution (40% methanol, 10% acetic acid, 0.25% Coomassie brilliant blue R-250) and de-stained in distilled water. The gelatinolytic activity was visualized as a clear band against a blue background. ImageJ software was used to determine the size and intensity of each band.

The in situ gelatinolytic activity was measured using the EnzChek Gelatinase Assay kit (Molecular Probes). Frozen tissue sections from mouse corneas (10 μm thick) in optimal cutting temperature compound were incubated with 50 $\mu\text{g/ml}$ DQ-gelatin-fluorescein isothiocyanate for 3 h at 37°C. After washing with PBS, the sections were mounted using coverslips and VectaShield mounting medium containing DAPI. As a negative control, the sections were incubated with reaction buffer supplemented with a general metalloproteinase inhibitor (1,10-phenanthroline, 1 mM). Images were captured with a 20x objective lens on a Zeiss Axio Observer Z1 inverted fluorescence microscope.

Immunoblotting

Protein from cell cultures was extracted using a buffer containing 150 mM NaCl, 50 mM Tris-HCl, pH 8.0, 1% Triton X-100, 5 mM EDTA and 1 mM PMSF supplemented with Complete™ Protease Inhibitor Cocktail (Roche Diagnostics). After homogenization with a pellet pestle, the protein cell extracts were centrifuged at 13,000 g for 45 min, and the protein concentration of the supernatant determined using the Pierce BCA™ Protein Assay Kit (Thermo Fisher Scientific). Proteins in cell lysates (15 μg) were resolved in 10% SDS-PAGE, and electroblotted onto nitrocellulose membranes (Bio-Rad). Membranes were then incubated with primary antibodies against galectin-3 (1 $\mu\text{g/ml}$; sc20157, Santa Cruz

Biotechnology), caveolin-1 (1 µg/ml; C3237, Sigma-Aldrich) and GAPDH (1 µg/ml; sc25778, Santa Cruz Biotechnology) in TBST for 2 h at room temperature, followed by the appropriate secondary antibodies coupled to horseradish peroxidase (Santa Cruz Biotechnology). Peroxidase activity was detected using the G:BOX Chemi XRQ (Syngene). Band intensities were quantified by densitometry using ImageJ software.

Dissected corneas from enucleated mouse eyes were treated with 30 mM EDTA for 30 min at 37°C to remove the epithelial sheet (46). Corneas from three mice in each group were pooled and homogenized in lysis buffer (150 mM NaCl, 50 mM Tris-HCl, pH 8.0, 0.5% Triton X-100, 1 mM PMSF) supplemented with Complete™ Protease Inhibitor Cocktail, using three sonication rounds (10 sec per round) followed by five freeze/thaw cycles. Samples were centrifuged at 13,000 g for 30 min and the supernatants concentrated using Amicon Ultra centrifugal filters (10 kD). Proteins in the lysates were resolved in 10% SDS-PAGE, and electroblotted onto nitrocellulose membranes. Membranes were then incubated with primary antibodies against IL1β/IL1F2 (1 µg/ml; MAB401, R&D Systems), galectin-3 (undiluted hybridoma supernatant; M3/38 clone) and β-actin (1 µg/ml; 8H10D10, Cell Signaling Technology) followed by the appropriate secondary antibodies. Band intensities were quantified by densitometry using ImageJ software.

RNA Isolation and cDNA synthesis

Total RNA was isolated using the extraction reagent TRIzol (Thermo Fisher Scientific) following the manufacturer's instructions. Residual genomic DNA in the RNA preparation was eliminated by amplification-grade DNase I (Invitrogen). RNA concentration and purity was assessed using a NanoDrop 2000 spectrophotometer (Thermo Fisher Scientific). The concentration of RNA was calculated at 260nm, and the ratio of A_{260}/A_{280} was greater than 1.8. First strand cDNA was synthesized from 1 µg (for qPCR) or 3 µg (for PCR array) total RNA using the iScript™ cDNA synthesis kit (Bio-Rad) in a 25-µl reaction volume according to the manufacturer's instructions.

qPCR and PCR Array

Gene expression was determined by quantitative real-time PCR using the SsoAdvanced™ Universal SYBR® Green Supermix (Bio-Rad) in a Mastercycler RealPlex 2 (Eppendorf). Primers for *MMP9* (cat. no. qHsaCID0011597) and *GAPDH* (cat. no. qHsaCED0038674) were obtained from Bio-Rad. The following parameters were used: 2 minutes at 95°C, followed by 40 cycles of 5 seconds at 95°C and 30 seconds at 60°C. All samples were normalized using *GAPDH* housekeeping gene expression. The comparative 2^{-CT} method was used for relative quantitation of the number of transcripts. No-template controls were run in each assay to confirm lack of DNA contamination in the reagents used for amplification.

The analysis of 84 genes involved in autoimmune and inflammatory immune responses was carried out using a human RT² Profiler PCR Array (PAHS-077Z; Qiagen) according to the manufacturer's instructions. Cells were incubated for 24 h in DMEM/F12 serum-free medium before RNA Isolation and cDNA synthesis. The array was repeated three times with independently isolated RNA. All samples were normalized using *RPLP0* housekeeping gene

expression. The 2^{-CT} and 2^{-CT} methods were used for relative quantitation of the number of transcripts.

RNA Interference

Depletion of either galectin-3 (ID s8149) or IL1 β (ID s223930) was achieved using Silencer® Select siRNAs (Life Technologies). A non-targeting scrambled siRNA (ID 4390843) served as negative control. For knockdown, cells were transfected by a 6-h incubation with 500 nM siRNA in Lipofectamine 2000 (0.5 μ l/100 mm², Life Technologies) dissolved in Opti-MEM reduced-serum medium (Life Technologies). Levels of galectin-3 or IL1 β were determined by immunoblot and ELISA, respectively, 72 h after siRNA transfection.

Production of Recombinant Galectin-3

Full-length galectin-3 and a galectin-3 N-terminal deletion mutant were produced as previously described (47). Heterologous protein expression was induced in Rosetta *E. coli* clones by addition of 0.3 mM IPTG. The proteins were purified from lysates by affinity chromatography using lactosyl sepharose. To eliminate contaminating bacterial endotoxins, the proteins were further purified by polymyxinB affinity chromatography (Sigma-Aldrich). The absence of lipopolysaccharide was confirmed using the ToxinSensor™ Chromogenic LAL Endotoxin Assay Kit (GenScript). Protein solutions were concentrated by centrifugal filtration (VWR), dialyzed against PBS buffer containing 10% glycerol and stored at -20°C .

ELISA

Conditioned media from cells incubated for 24 h in serum-free conditions were collected and centrifuged at 13,000 g for 30 min to remove cells and cellular debris. Supernatants were analyzed for IL1 β and CXCL10 concentrations using ELISA Max™ kits (Biolegend) according to the manufacturer's instructions.

Plasma Membrane Protein Extraction

Primary cultures of human corneal fibroblasts were fractionated using a Plasma Membrane Protein Extraction kit (Abcam) according to the manufacturer's instructions.

Supplementary Material

Refer to Web version on PubMed Central for supplementary material.

Acknowledgments:

The authors thank Ilene K. Gipson and James V. Jester for providing the human corneal epithelial and human fibroblast cell lines, respectively. We also thank Miguel Gonzalez-Andrades for assistance in providing corneal donor tissue samples and Ashley M. Woodward, Anokhi Kapasi Sullivan, Sharad Mittal, and Oscar Morales for assistance in the technical development of the project.

Funding: This work was supported by the National Institutes of Health, NEI Grant R01EY024031 (P.A.) and NEI Core Grant P30EY003790.

REFERENCES AND NOTES

1. Bogenrieder T, Herlyn M, Axis of evil: molecular mechanisms of cancer metastasis. *Oncogene* 22, 6524–6536 (2003). [PubMed: 14528277]
2. Ingber DE, Cancer as a disease of epithelial-mesenchymal interactions and extracellular matrix regulation. *Differentiation* 70, 547–560 (2002). [PubMed: 12492496]
3. Bergers G, Coussens LM, Extrinsic regulators of epithelial tumor progression: metalloproteinases. *Curr Opin Genet Dev* 10, 120–127 (2000). [PubMed: 10679388]
4. Yao PM, Buhler JM, d'Ortho MP, Lebargy F, Delclaux C, Harf A, Lafuma C, Expression of matrix metalloproteinase gelatinases A and B by cultured epithelial cells from human bronchial explants. *J Biol Chem* 271, 15580–15589 (1996). [PubMed: 8663061]
5. Loffek S, Schilling O, Franzke CW, Series “matrix metalloproteinases in lung health and disease”: Biological role of matrix metalloproteinases: a critical balance. *Eur Respir J* 38, 191–208 (2011). [PubMed: 21177845]
6. Van den Steen PE, Dubois B, Nelissen I, Rudd PM, Dwek RA, Opdenakker G, Biochemistry and molecular biology of gelatinase B or matrix metalloproteinase-9 (MMP-9). *Crit Rev Biochem Mol Biol* 37, 375–536 (2002). [PubMed: 12540195]
7. LeBert DC, Squirrell JM, Rindy J, Broadbridge E, Lui Y, Zakrzewska A, Eliceiri KW, Meijer AH, Huttenlocher A, Matrix metalloproteinase 9 modulates collagen matrices and wound repair. *Development* 142, 2136–2146 (2015). [PubMed: 26015541]
8. Kyriakides TR, Wulsin D, Skokos EA, Fleckman P, Pirrone A, Shipley JM, Senior RM, Bornstein P, Mice that lack matrix metalloproteinase-9 display delayed wound healing associated with delayed reepithelization and disordered collagen fibrillogenesis. *Matrix Biol* 28, 65–73 (2009). [PubMed: 19379668]
9. Mohan R, Chintala SK, Jung JC, Villar WV, McCabe F, Russo LA, Lee Y, McCarthy BE, Wollenberg KR, Jester JV, Wang M, Welgus HG, Shipley JM, Senior RM, Fini ME, Matrix metalloproteinase gelatinase B (MMP-9) coordinates and effects epithelial regeneration. *J Biol Chem* 277, 2065–2072 (2002). [PubMed: 11689563]
10. Matsubara M, Zieske JD, Fini ME, Mechanism of basement membrane dissolution preceding corneal ulceration. *Invest Ophthalmol Vis Sci* 32, 3221–3237 (1991). [PubMed: 1660857]
11. Lau KS, Partridge EA, Grigorian A, Silvescu CI, Reinhold VN, Demetriou M, Dennis JW, Complex N-glycan number and degree of branching cooperate to regulate cell proliferation and differentiation. *Cell* 129, 123–134 (2007). [PubMed: 17418791]
12. Argueso P, Mauris J, Uchino Y, Galectin-3 as a regulator of the epithelial junction: Implications to wound repair and cancer. *Tissue Barriers* 3, e1026505 (2015). [PubMed: 26451339]
13. Fortuna-Costa A, Gomes AM, Kozłowski EO, Stelling MP, Pavao MS, Extracellular galectin-3 in tumor progression and metastasis. *Front Oncol* 4, 138 (2014). [PubMed: 24982845]
14. Elenbaas B, Weinberg RA, Heterotypic signaling between epithelial tumor cells and fibroblasts in carcinoma formation. *Exp Cell Res* 264, 169–184 (2001). [PubMed: 11237532]
15. Breznik B, Motaln H, Lah Turnsek T, Proteases and cytokines as mediators of interactions between cancer and stromal cells in tumours. *Biol Chem* 398, 709–719 (2017). [PubMed: 28002021]
16. Nieminen J, Kuno A, Hirabayashi J, Sato S, Visualization of galectin-3 oligomerization on the surface of neutrophils and endothelial cells using fluorescence resonance energy transfer. *J Biol Chem* 282, 1374–1383 (2007). [PubMed: 17082191]
17. Gordon GM, Ledee DR, Feuer WJ, Fini ME, Cytokines and signaling pathways regulating matrix metalloproteinase-9 (MMP-9) expression in corneal epithelial cells. *J Cell Physiol* 221, 402–411 (2009). [PubMed: 19626678]
18. Morrissey MA, Sherwood DR, An active role for basement membrane assembly and modification in tissue sculpting. *J Cell Sci* 128, 1661–1668 (2015). [PubMed: 25717004]
19. Stepp MA, Zieske JD, Trinkaus-Randall V, Kyne BM, Pal-Ghosh S, Tadvalkar G, Pajoohesh-Ganji A, Wounding the cornea to learn how it heals. *Exp Eye Res* 121, 178–193 (2014). [PubMed: 24607489]
20. Wilson SE, Chaurasia SS, Medeiros FW, Apoptosis in the initiation, modulation and termination of the corneal wound healing response. *Exp Eye Res* 85, 305–311 (2007). [PubMed: 17655845]

21. Grillo HC, Gross J, Collagenolytic activity during mammalian wound repair. *Dev Biol* 15, 300–317 (1967). [PubMed: 4291909]
22. Sevenich L, Joyce JA, Pericellular proteolysis in cancer. *Genes Dev* 28, 2331–2347 (2014). [PubMed: 25367033]
23. Sengupta N, MacDonald TT, The role of matrix metalloproteinases in stromal/epithelial interactions in the gut. *Physiology (Bethesda)* 22, 401–409 (2007). [PubMed: 18073413]
24. Chang C, Werb Z, The many faces of metalloproteases: cell growth, invasion, angiogenesis and metastasis. *Trends Cell Biol* 11, S37–43 (2001). [PubMed: 11684441]
25. Zhao W, Ajani JA, Sushovan G, Ochi N, Hwang R, Hafley M, Johnson RL, Bresalier RS, Logsdon CD, Zhang Z, Song S, Galectin-3 Mediates Tumor Cell-Stroma Interactions by Activating Pancreatic Stellate Cells to Produce Cytokines via Integrin Signaling. *Gastroenterology* 154, 1524–1537 e1526 (2018). [PubMed: 29274868]
26. Weng J, Mohan RR, Li Q, Wilson SE, IL-1 upregulates keratinocyte growth factor and hepatocyte growth factor mRNA and protein production by cultured stromal fibroblast cells: interleukin-1 beta expression in the cornea. *Cornea* 16, 465–471 (1997). [PubMed: 9220246]
27. Kennedy MC, Rosenbaum JT, Brown J, Planck SR, Huang X, Armstrong CA, Ansel JC, Novel production of interleukin-1 receptor antagonist peptides in normal human cornea. *J Clin Invest* 95, 82–88 (1995). [PubMed: 7814649]
28. Uchino Y, Woodward AM, Mauris J, Peterson K, Verma P, Nilsson UJ, Rajaiya J, Argueso P, Galectin-3 is an amplifier of the interleukin-1beta-mediated inflammatory response in corneal keratinocytes. *Immunology* 154, 490–499 (2018). [PubMed: 29359328]
29. Sugioka K, Mishima H, Kodama A, Itahashi M, Fukuda M, Shimomura Y, Regulatory Mechanism of Collagen Degradation by Keratocytes and Corneal Inflammation: The Role of Urokinase-Type Plasminogen Activator. *Cornea* 35 Suppl 1, S59–S64 (2016). [PubMed: 27661072]
30. Barbosa FL, Chaurasia SS, Kaur H, de Medeiros FW, Agrawal V, Wilson SE, Stromal interleukin-1 expression in the cornea after haze-associated injury. *Exp Eye Res* 91, 456–461 (2010). [PubMed: 20603114]
31. Filer A, Bik M, Parsonage GN, Fitton J, Trebilcock E, Howlett K, Cook M, Raza K, Simmons DL, Thomas AM, Salmon M, Scheel-Toellner D, Lord JM, Rabinovich GA, Buckley CD, Galectin 3 induces a distinctive pattern of cytokine and chemokine production in rheumatoid synovial fibroblasts via selective signaling pathways. *Arthritis Rheum* 60, 1604–1614 (2009). [PubMed: 19479862]
32. Arad U, Madar-Balakirski N, Angel-Korman A, Amir S, Tzadok S, Segal O, Menachem A, Gold A, Elkayam O, Caspi D, Galectin-3 is a sensor-regulator of toll-like receptor pathways in synovial fibroblasts. *Cytokine* 73, 30–35 (2015). [PubMed: 25689620]
33. Lippert E, Falk W, Bataille F, Kaehne T, Naumann M, Goeke M, Herfarth H, Schoelmerich J, Rogler G, Soluble galectin-3 is a strong, colonic epithelial-cell-derived, lamina propria fibroblast-stimulating factor. *Gut* 56, 43–51 (2007). [PubMed: 16709662]
34. Inohara H, Akahani S, Raz A, Galectin-3 stimulates cell proliferation. *Exp Cell Res* 245, 294–302 (1998). [PubMed: 9851870]
35. Partridge EA, Le Roy C, Di Guglielmo GM, Pawling J, Cheung P, Granovsky M, Nabi IR, Wrana JL, Dennis JW, Regulation of cytokine receptors by Golgi N-glycan processing and endocytosis. *Science* 306, 120–124 (2004). [PubMed: 15459394]
36. Clark MC, Pang M, Hsu DK, Liu FT, de Vos S, Gascoyne RD, Said J, Baum LG, Galectin-3 binds to CD45 on diffuse large B-cell lymphoma cells to regulate susceptibility to cell death. *Blood* 120, 4635–4644 (2012). [PubMed: 23065155]
37. Carlow DA, Williams MJ, Ziltener HJ, Modulation of O-glycans and N-glycans on murine CD8 T cells fails to alter annexin V ligand induction by galectin 1. *J Immunol* 171, 5100–5106 (2003). [PubMed: 14607908]
38. Boscher C, Zheng YZ, Lakshminarayan R, Johannes L, Dennis JW, Foster LJ, Nabi IR, Galectin-3 protein regulates mobility of N-cadherin and GM1 ganglioside at cell-cell junctions of mammary carcinoma cells. *J Biol Chem* 287, 32940–32952 (2012). [PubMed: 22846995]

39. Argueso P, Guzman-Aranguez A, Mantelli F, Cao Z, Ricciuto J, Panjwani N, Association of cell surface mucins with galectin-3 contributes to the ocular surface epithelial barrier. *J Biol Chem* 284, 23037–23045 (2009). [PubMed: 19556244]
40. Yu LG, Andrews N, Zhao Q, McKean D, Williams JF, Connor LJ, Gerasimenko OV, Hilken J, Hirabayashi J, Kasai K, Rhodes JM, Galectin-3 interaction with Thomsen-Friedenreich disaccharide on cancer-associated MUC1 causes increased cancer cell endothelial adhesion. *J Biol Chem* 282, 773–781 (2007). [PubMed: 17090543]
41. Guo X, Hutcheon AE, Melotti SA, Zieske JD, Trinkaus-Randall V, Ruberti JW, Morphologic characterization of organized extracellular matrix deposition by ascorbic acid-stimulated human corneal fibroblasts. *Invest Ophthalmol Vis Sci* 48, 4050–4060 (2007). [PubMed: 17724187]
42. Gipson IK, Spurr-Michaud S, Argueso P, Tisdale A, Ng TF, Russo CL, Mucin gene expression in immortalized human corneal-limbal and conjunctival epithelial cell lines. *Invest Ophthalmol Vis Sci* 44, 2496–2506 (2003). [PubMed: 12766048]
43. Jester JV, Huang J, Fisher S, Spiekerman J, Chang JH, Wright WE, Shay JW, Myofibroblast differentiation of normal human keratocytes and hTERT, extended-life human corneal fibroblasts. *Invest Ophthalmol Vis Sci* 44, 1850–1858 (2003). [PubMed: 12714615]
44. Pal-Ghosh S, Pajoohesh-Ganji A, Tadvalkar G, Stepp MA, Removal of the basement membrane enhances corneal wound healing. *Exp Eye Res* 93, 927–936 (2011). [PubMed: 22067129]
45. Bogdanowicz DR, Lu HH, Multifunction co-culture model for evaluating cell-cell interactions. *Methods Mol Biol* 1202, 29–36 (2014). [PubMed: 24504928]
46. Spurr SJ, Gipson IK, Isolation of corneal epithelium with Dispase II or EDTA. Effects on the basement membrane zone. *Invest Ophthalmol Vis Sci* 26, 818–827 (1985). [PubMed: 3924852]
47. Mauris J, Mantelli F, Woodward AM, Cao Z, Bertozzi CR, Panjwani N, Godula K, Argueso P, Modulation of ocular surface glycocalyx barrier function by a galectin-3 N-terminal deletion mutant and membrane-anchored synthetic glycopolymers. *PLoS One* 8, e72304 (2013). [PubMed: 23977277]

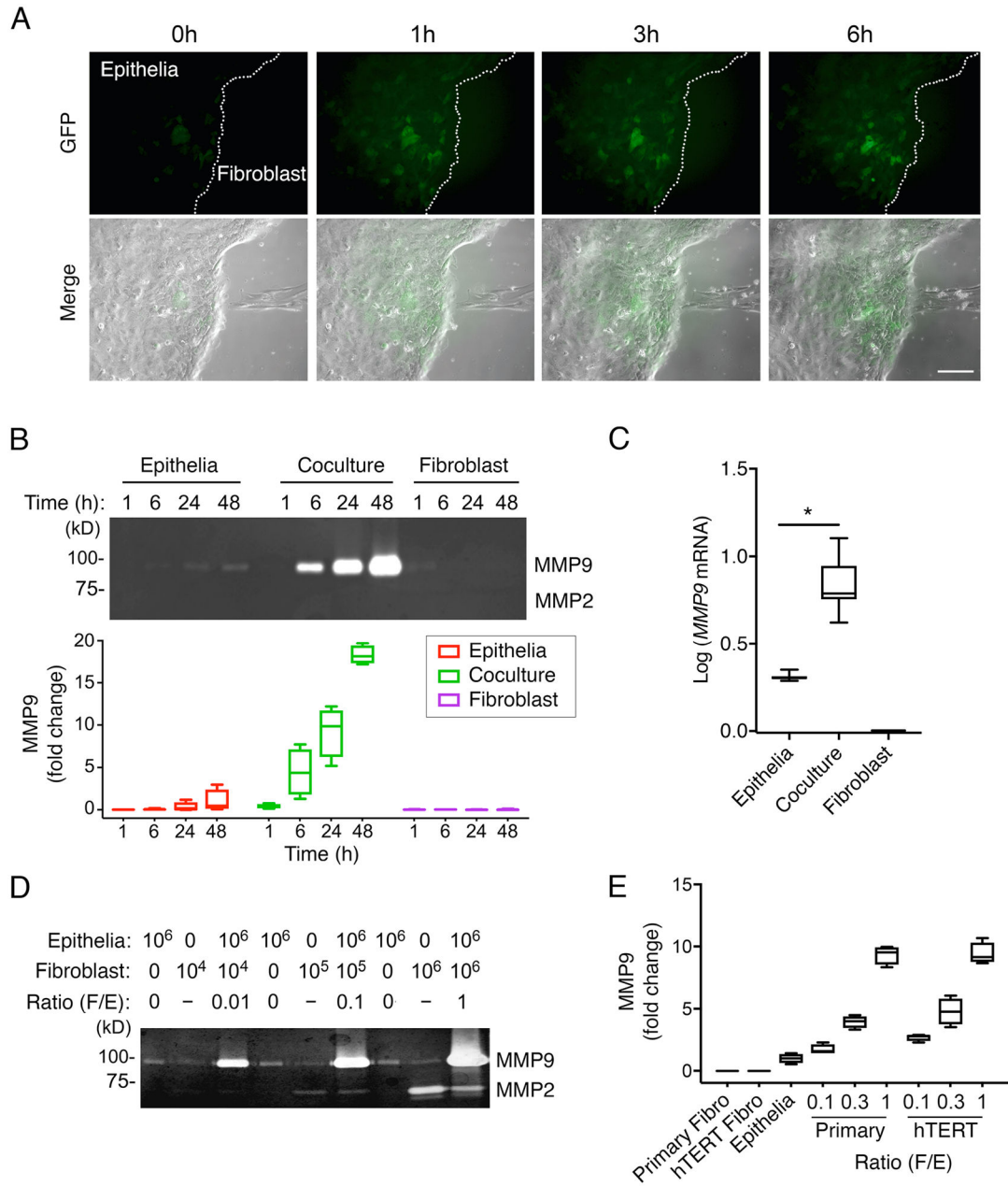


Fig. 1. MMP9 is locally activated in epithelial cells as a result of direct contact with fibroblasts. (A) Time-lapse phase-contrast and fluorescence images of immortalized human corneal epithelial cells carrying the *MMP9*-eGFP reporter construct and primary human corneal fibroblasts. (B) Gelatin zymography of culture media from epithelial cells and fibroblasts grown alone or in a mixed coculture system, in time course experiments. n = 4 independent experiments. (C) qPCR analysis of *MMP9* expression in cells grown alone or in coculture for 24 h. n = 8 independent experiments. (D) Gelatin zymography showing MMP activity with increasing numbers of fibroblasts relative to epithelial cells in coculture for 24 h. n = 3 independent experiments. (E) Gelatin zymography of culture media from cells grown alone or in coculture using immortalized human corneal epithelial cells and either primary human

corneal fibroblasts or telomerase-immortalized human corneal fibroblasts (hTERT). $n = 4$ independent experiments. The box and whisker plots show the 25 and 75 percentiles (box), the median (horizontal line in box), and the minimum and maximum data values (whiskers). Significance was determined using the Wilcoxon test. *, $p < 0.05$. Scale bar, 250 μm .

Author Manuscript

Author Manuscript

Author Manuscript

Author Manuscript

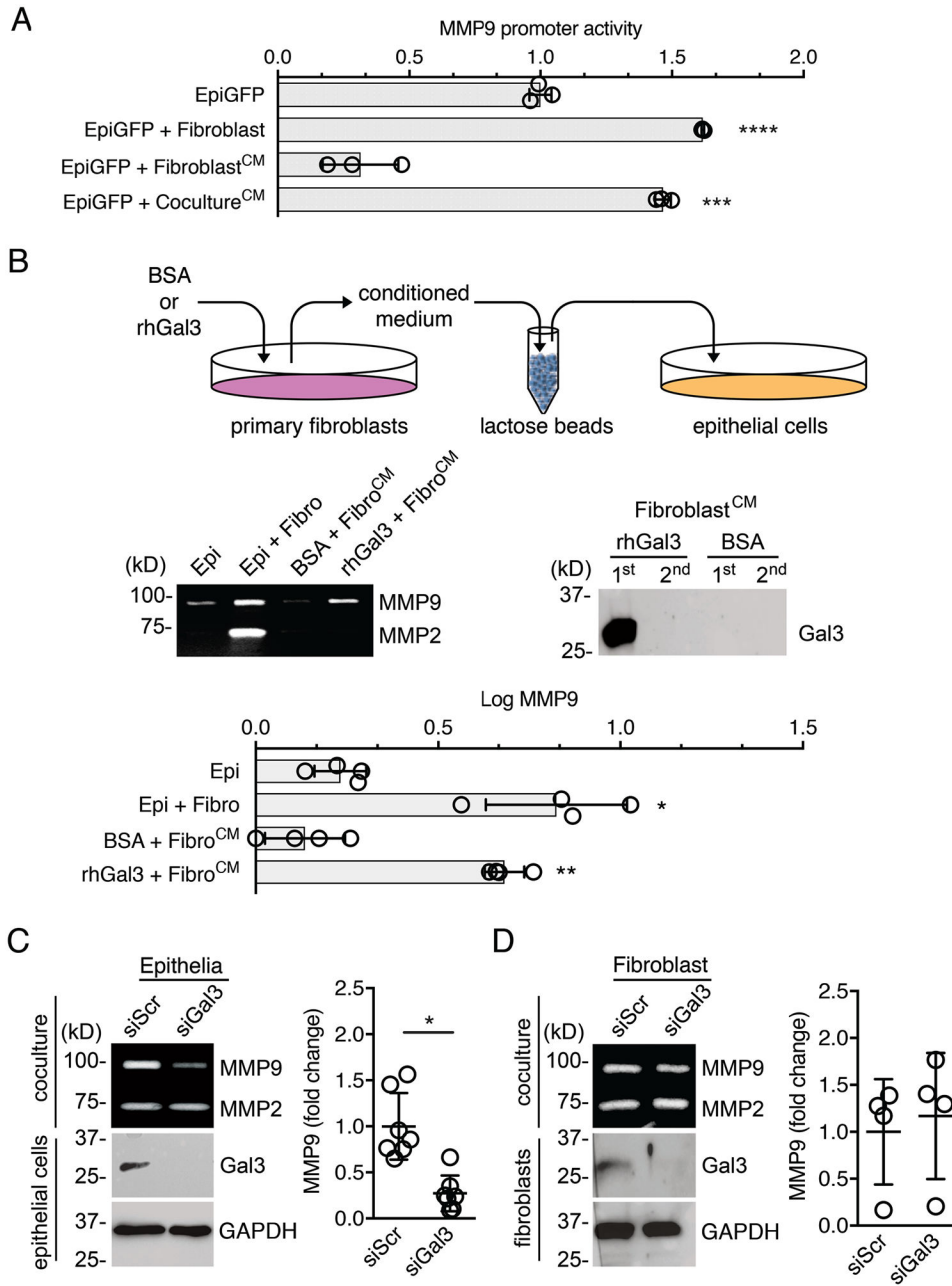


Fig. 2. Galectin-3 stimulates reciprocal signaling and influences epithelial MMP9 secretion. (A) Fluorescence intensity measured in human corneal epithelial cells carrying the *MMP9* reporter construct (EpiGFP). The serum-free conditioned media (CM) of fibroblasts grown alone or in coculture with epithelial cells for 24 h were diluted in a 1:1 ratio with fresh media and used to stimulate homotypic cultures of EpiGFP cells for an additional 24 h. n = 3 independent experiments. (B) Exogenous soluble galectin-3 (rhGal3) or BSA in serum-free media were incubated with fibroblasts for 24 h. The conditioned media were pre-cleared with α -lactose agarose beads to remove galectin-3 prior to incubation with epithelial cells. After an additional 24 h, the epithelial cell culture supernatants were analyzed by gelatin zymography to determine the abundance of MMP9. The presence of galectin-3 in pre-

cleared conditioned media was evaluated by immunoblotting. n = 4 independent experiments. **(C)** Epithelial cells were transfected with scrambled (siScr) or galectin-3 (siGal3) siRNA, and the presence of galectin-3 in epithelial cell lysates was assessed by immunoblotting. After 48h of transfection, cells were incubated with fibroblasts in a mixed coculture system for an additional 24 h. MMP9 abundance in the media was quantified by gelatin zymography and shown as a scatter plot. n = 7 independent experiments. **(D)** Same as (C) except that galectin-3 was knocked down in fibroblasts (siGal3) that were then cocultured with epithelial cells. n = 4 independent experiments. The data represent the mean \pm S.D. Significance was determined using one-way ANOVA with Tukey's post hoc test (A, B) or the Wilcoxon test (C, D). *, p<0.05; **, p<0.01; ***, p<0.001; ****, p<0.0001.

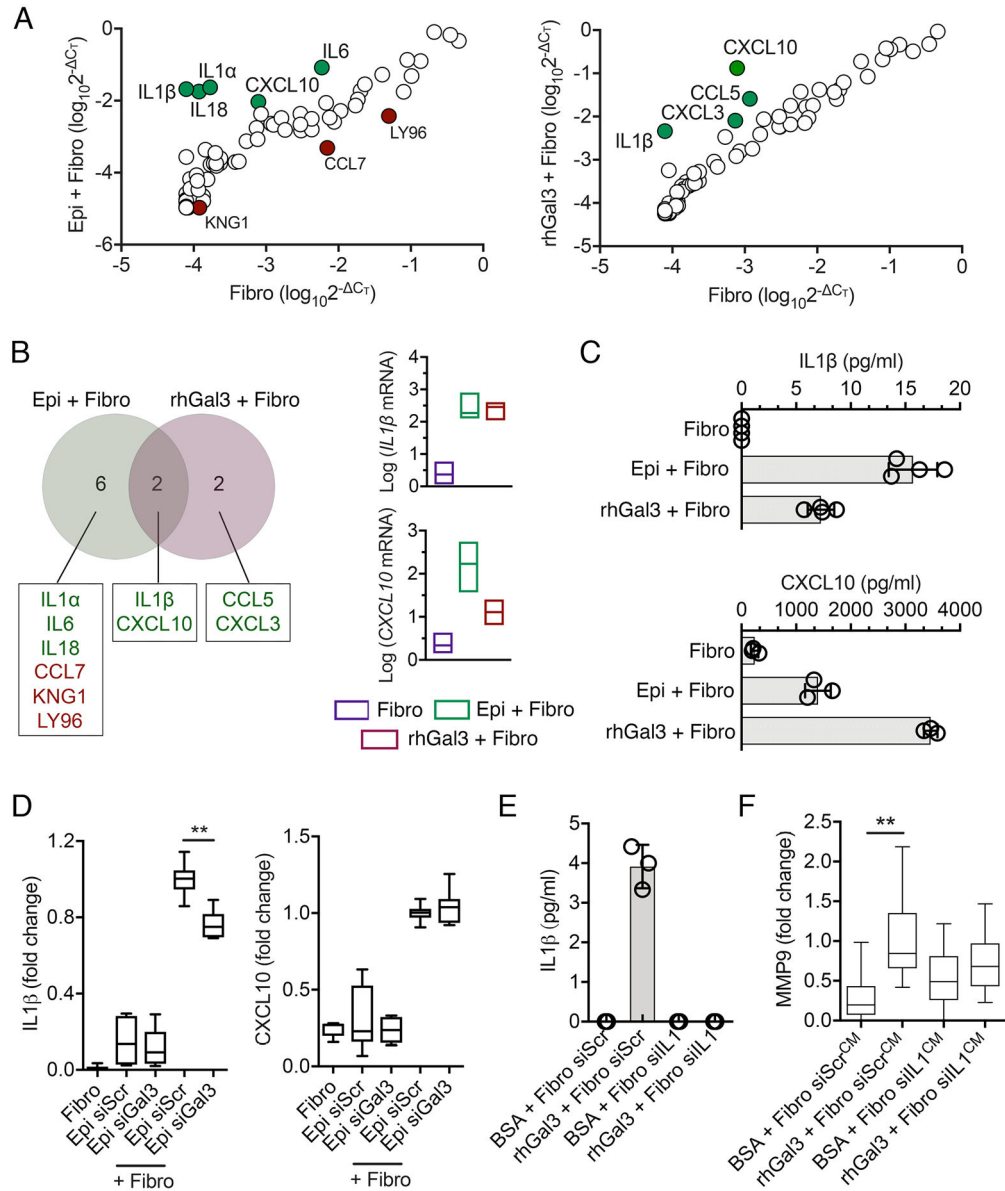


Fig. 3. IL-1 β acts as a galectin-3-induced paracrine signal in fibroblasts.
(A) Relative gene expression from PCR arrays on a mixed coculture system (Epi + Fibro) or fibroblasts exposed to exogenous soluble galectin-3 (rhGal3 + Fibro) for 24 h. Data were normalized to cultures of fibroblasts grown alone with no stimulation. The green and red dots indicate significant increases or decreases compared to the control, respectively. n = 3 independent experiments. **(B)** Venn diagram representation of genes showing increased and decreased expression in coculture conditions or in fibroblasts exposed to galectin-3, as determined by PCR array. The expression amounts of the two overlapping genes are shown for each individual condition. n = 3 independent experiments. **(C)** ELISA showing the amounts of IL-1 β and CXCL10 in culture supernatants obtained from the conditions in (A). n = 4 (IL-1 β) or n = 3 (CXCL10) independent experiments. **(D)** Epithelial cells were transfected with scrambled (siScr) or galectin-3 (siGal3) siRNA. After 48h of transfection,

cells were incubated with fibroblasts in a mixed coculture system for an additional 24 h. IL-1 β and CXCL10 amounts in culture supernatants were quantified by ELISA. n = 6 independent experiments. **(E)** Fibroblasts were transfected with siScr or IL-1 β siRNA (siIL1). After 48h of transfection, cells were incubated with BSA or rhGal3 in serum-free media for an additional 24 h. IL-1 β amounts in culture supernatants were quantified by ELISA. n = 3 independent experiments. **(F)** Culture supernatants obtained from the conditions in (E) were pre-cleared twice with α -lactose agarose beads to remove endogenous galectin-3 prior to incubation with epithelial cells. After 24 h, the gelatinase (MMP9) activity of epithelial cell culture supernatants was quantified by gelatin zymography. n = 4 independent experiments. The box and whisker plots show the 25 and 75 percentiles (box), the median, and the minimum and maximum data values (whiskers). The data in (C) and (E) represent the mean \pm S.D. Significance was determined using one-way ANOVA with Tukey's post hoc test. **, p<0.01.

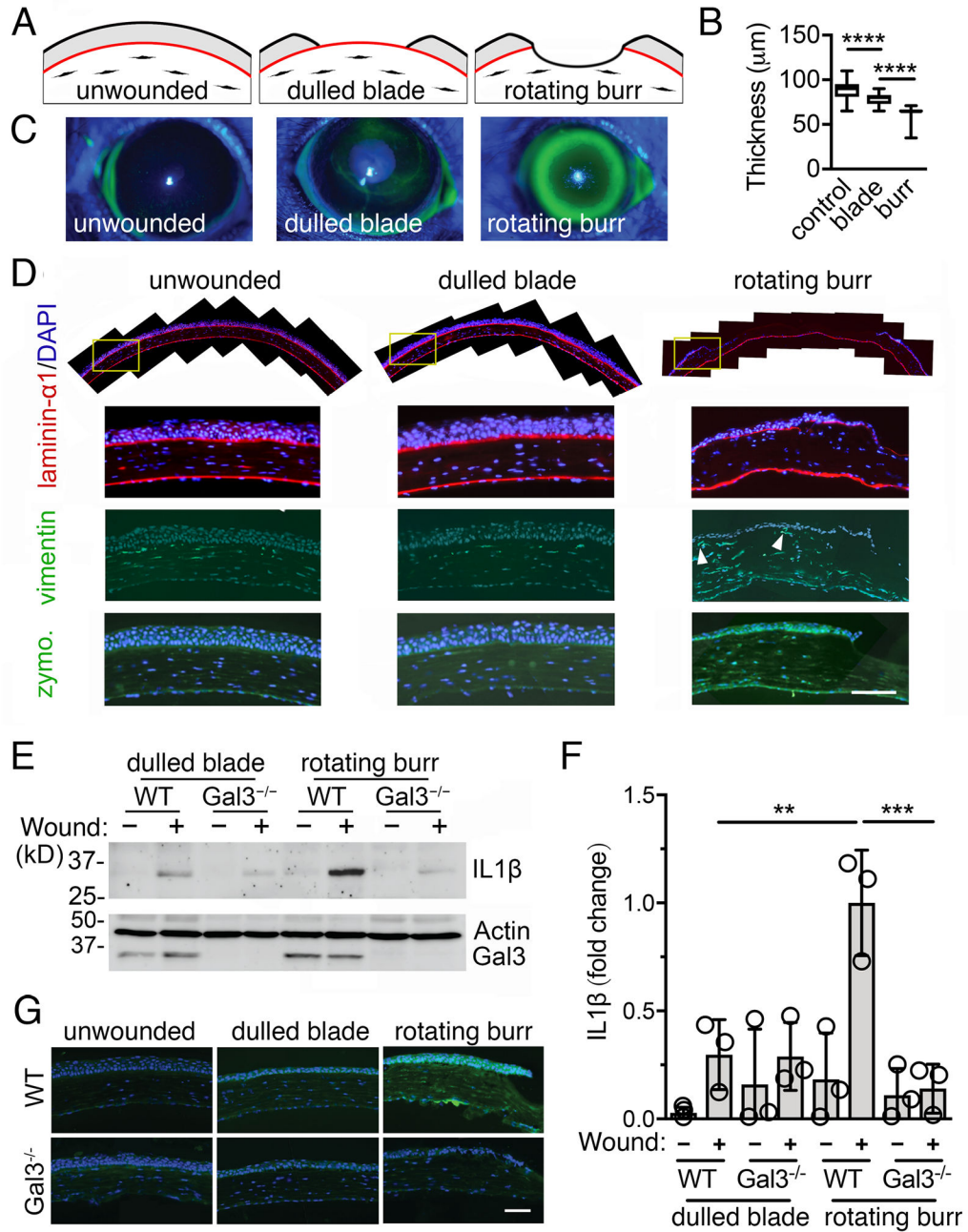


Fig. 4. The basement membrane protects against galectin-3-induced IL-1 β signaling. (A) Schematic representation of the two models of corneal injury used in this study. (B) The corneal thickness was determined immediately after wounding by anterior segment optical coherence tomography. $n =$ at least 19 eyes from 19 mice per group. (C) Re-epithelialization was monitored after 14–16 h using fluorescein, which stains areas where the epithelium is absent or damaged. (D) Control and wounded corneas were harvested 14–16 h after injury and subjected to immunofluorescence for laminin- α 1 (red; localizes to basement membranes) and vimentin (green; present in mesenchymal cells). Nuclei were stained by DAPI (blue). Fibroblasts in close proximity to the epithelium are noted with arrowheads.

The gelatinolytic activity in these samples was assessed by in situ zymography. Data is representative of 2 independent experiments. **(E)** The presence of IL-1 β , galectin-3, and β -actin in de-epithelialized corneas from wild-type (WT) and galectin-3-deficient (Gal3^{-/-}) mice was evaluated by immunoblotting. n = 3 independent experiments using 3 corneas per group. A representative blot is shown. **(F)** ImageJ quantification of IL-1 β staining shown in **(E)**. n = 3 independent experiments. **(G)** The gelatinolytic activity in WT and galectin-3-deficient mice was assessed by in situ zymography. The box and whisker plots show the 25 and 75 percentiles (box), the median, and the minimum and maximum data values (whiskers). The data in **(F)** represent the mean \pm S.D. Significance was determined using one-way ANOVA with Tukey's post hoc test. **, p<0.01; ***, p<0.001; ****, p<0.0001. Scale bars, 100 μ m.

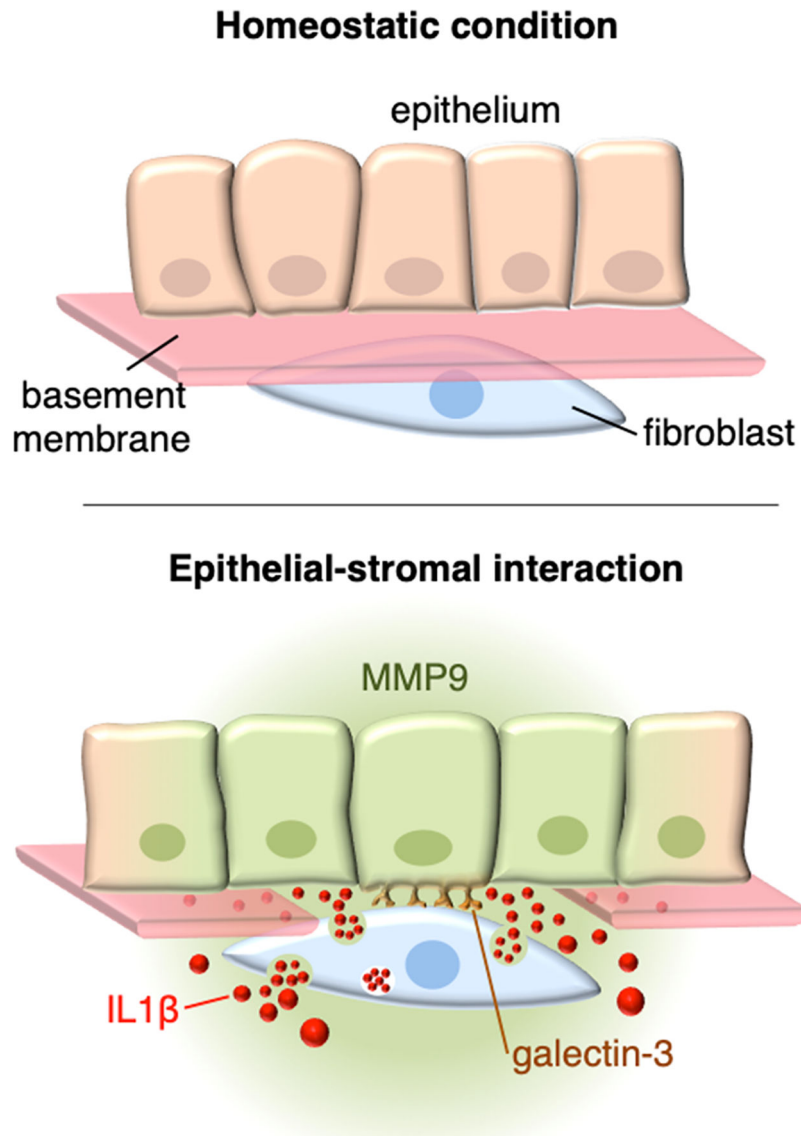


Fig. 5. Mechanism of galectin-3-induced paracrine signaling in epithelial-stromal interactions. Multiple functions have been ascribed to the basement membrane, a thin and highly cross-linked extracellular matrix that underlies all epithelia. During homeostatic conditions, these include promotion of mechanical strength, and the maintenance of tissue architecture. Disruption of the basement membrane by trauma allows for direct interactions between epithelial cells and stromal fibroblasts, resulting in a cascade of signaling events critical for tissue repair. We propose that galectin-3 of epithelial origin initiates such events by physically interacting with fibroblasts through an as yet unidentified receptor. As a consequence, the stromal fibroblasts begin to synthesize and secrete abundant amounts of IL-1 β , which act in a paracrine fashion to regulate the proteolytic microenvironment by activating the *MMP9* promoter in epithelial cells. This reciprocal form of communication would be expected to lead to the remodeling of the collagenous extracellular matrix.